



## Mantle conveyor beneath the Tethyan collisional belt

Thorsten W. Becker <sup>a,\*</sup>, Claudio Faccenna <sup>b</sup>

<sup>a</sup> Department of Earth Sciences, University of Southern California, Los Angeles, CA, USA

<sup>b</sup> Dipartimento Scienze Geologiche, Università Roma TRE and IGAG, CNR, Rome

### ARTICLE INFO

#### Article history:

Received 28 April 2011

Received in revised form 5 August 2011

Accepted 12 August 2011

Available online xxxx

Editor: Y. Ricard

#### Keywords:

continental collision

mantle upwelling

plate motions

plate driving forces

### ABSTRACT

Collisional belts are generated by the arrival of continental lithosphere into a subduction zone. The Tethyan suture from the Bitlis to the Himalayas is a prime example where the Arabian and Indian plates collided with Eurasia during the Cenozoic. While the kinematics of this process are well established, its dynamics are more uncertain. India and Arabia intriguingly keep advancing, in spite of large collisional resisting forces, and in the absence of a substantial, upper mantle slab driving force at present-day. We perform global mantle circulation computations to test the role of deep mantle flow as a driving force for the kinematics of the Tethyan collisional belt, evaluating different boundary conditions and mantle density distributions as inferred from seismic tomography or slab models. Our results show that mantle drag exerted on the base of the lithosphere by a large-scale, convective “conveyor belt” with an active upwelling component is likely the main cause for the ongoing indentation of the Indian and Arabian plates into Eurasia.

© 2011 Elsevier B.V. All rights reserved.

## 1. Introduction

Collisional orogens are among the most impressive manifestations of plate tectonics. The classical theory for orogeny suggests that crustal thickening persists after the entrance of continental lithosphere at the trench and ceases when the driving pull of the subducting oceanic lithosphere vanishes, e.g. after detachment of the slab (Cloos, 1993). However, along the Himalayas, collision was sustained over most of the Cenozoic. The Indian plate was pushed into Asia, over ~600 to 1000 km, forming the Tibetan plateau and the Tien Shan (Johnson, 2002; van Hinsbergen et al., in press; Yin and Harrison, 2000). On a smaller scale and at a reduced rate, Arabia also advanced into Eurasia, creating the Bitlis-Zagros collisional belt during the spreading of the Red Sea-Gulf of Aden ocean (Hatzfeld and Molnar, 2010; McQuarrie et al., 2003). A longstanding, but not entirely resolved question then concerns the driving forces for the northward motion of Arabia and India, which has to be sufficient to overcome the large resistance of the collisional system over a long time span.

### 1.1. Kinematics in the present and past

Despite their differences in scale and rates, the present kinematic patterns associated with the motion of the India and Arabia plates with respect to fixed Eurasia show some striking similarities (Hatzfeld and Molnar, 2010). Separated via ridge systems from the

large and relatively slowly moving African continent, India and Arabia show northward indentation into Eurasia. On both plates, the geodetically inferred velocities decrease gradually inside the collision zone. Velocities then progressively turn laterally outward, in a toroidal flow fashion, toward active subduction zones: the Hellenic and the western Philippine Sea plate trenches for Arabia and the Indian plate, respectively.

The geological history of the two plates shares common features that can be associated with punctuated mantle upwellings on several occasions. India separated from Antarctica-Australia at ~125 Ma, associated with the Kerguelan Large Igneous Province (LIP) (Gaina et al., 2007), from Madagascar after the emplacement of the Morondova LIP (91–84 Ma; Torsvik et al., 2000), and from the Seychelles micro continent just after the Deccan LIP event (~65 Ma), related to the Réunion plume (Cande and Stegman, 2011; van Hinsbergen et al., 2011). During this period, India's plate motion increased up to the highest reliably recorded velocities (Patriat and Achache, 1984; Copley et al., 2010).

It is commonly inferred that continental India collided with Asia at ~50 Ma (Guillot et al., 2003; Hatzfeld and Molnar, 2010; Molnar and Tapponnier, 1975). After collision, India's plate velocity decreased, to ~4–5 cm/yr at the present day (Copley et al., 2010; Zhang et al., 2004). Between ~25% and 50% of the plate velocity during the last ~25 Ma was accommodated by overriding plate thickening and extrusion (van Hinsbergen et al., in press). The corresponding shortening rate of  $\lesssim 2$  cm/yr provides a lower bound for the long-term subduction velocity, and this collisional process may be associated with shallow dipping underthrusting of India's continental lithosphere below Tibet (Capitanio et al., 2010; Replumaz et al., 2010). Arabia broke apart from Africa at ~35 Ma, after the arrival of the

\* Corresponding author at: Department of Earth Sciences, University of Southern California, MC 0740, 3651 Trousdale Pkwy, Los Angeles, CA 90089-0740, USA. Tel.: +1 213 740 8365; fax: +1 213 740 8801.

E-mail address: [twb@usc.edu](mailto:twb@usc.edu) (T.W. Becker).

Afar plume (Ebinger and Sleep, 1998; McQuarrie et al., 2003). Continental underthrusting probably initiated at ~30 Ma while the current stage of collision initiated in the middle Miocene (~12 Ma) with a convergence rate of ~2.5 cm/yr (Allen and Armstrong, 2008; Hatzfeld and Molnar, 2010; Jolivet and Faccenna, 2000). It appears that Arabia's lateral motion was contemporaneous with continental underthrusting (Hatzfeld and Molnar, 2010; McQuarrie et al., 2003), and similar to the case of India, ~half of the present-day shortening is accommodated within the Zagros belt (ArRajehi et al., 2010; McClusky et al., 2003). Hence, the subduction velocity, corrected for overriding plate shortening, is likely  $\gtrsim 1.5$  cm/yr. We interpret the geologic record for the collisional system such that both convergence and subduction velocities decreased rapidly after continental collision, but then remained fairly constant over the last 20–30 Myrs. By inference, the present-day kinematics, for example as recorded by geodesy, may then be representative of the long-term force equilibrium (Meijer and Wortel, 1999).

## 1.2. Dynamics

Different classes of models have been proposed to understand the dynamics of the Tethyan collisional system. The first, and perhaps most popular, class of models proposes that the negative buoyancy force exerted by subduction of oceanic lithosphere (slab pull) may propel India and Arabia against Eurasia. This mechanism might also work for the case of continental subduction, provided that the buoyant, upper-crustal layers are scraped off from the lower crust and lithospheric mantle (Capitanio et al., 2010; Cloos, 1993). Laboratory and numerical models have reproduced the reduction of the subduction and convergence velocity by ratios similar to what is observed for India (Bellahsen et al., 2003; Capitanio et al., 2010; Chemenda et al., 2000). Slab pull probably represented an important force contribution during India's fast drift phase (Copley et al., 2010), modulating the decrease in the convergence motion (Capitanio et al., 2010; van Hinsbergen et al., 2011). However, at present, slab pull is expected to be reduced to its minimum level, given the inferred repeated episodes of slab break off (e.g. Chemenda et al., 2000; Faccenna et al., 2006; Hafkenscheid et al., 2006; Keskin, 2003; Replumaz et al., 2010).

Another important force contribution is represented by lithospheric thickening of the oceanic lithosphere (ridge push). Together with the pull force of the Tethyan subducting slab, ridge push has been considered as driving the indentation (Capitanio et al., 2010; Copley et al., 2010). Recent estimates of ridge push give values between 1 and  $2 \cdot 10^{12}$  N/m, however, which is too low to explain the deformation associated with the collisional system (Ghosh et al., 2006). Intraplate forcing transmitted from the surrounding plates, especially Indochina and Australia, could also contribute to explain the motion of the colliding plates (Cloetingh and Wortel, 1986; Coblenz et al., 1998; Flesch et al., 2005; Li et al., 2008a; Meijer and Wortel, 1999) given that the boundary between Australia and India is not well defined (e.g. Cande et al., 2010).

Lastly, a potential contribution is represented by the drag exerted by large scale mantle flow, a "continental undertow" (Alvarez, 1990). Mantle drag associated with regional, plume-like upwellings has been suggested as an efficient mechanism for rapid drift of continental plates, such as Laurentia or Baltica, when velocities are in excess of 10 cm/yr (Cande and Stegman, 2011; Gurnis and Torsvik, 1994; van Hinsbergen et al., 2011). The sustained convergence of the Tethyan belt may then be associated with a long-term drag exerted by larger-scale, whole mantle flow (Alvarez, 2010; Cande and Stegman, 2011; van Hinsbergen et al., 2011).

Here, we use global mantle flow computations to test the influence of different models of density anomalies within the mantle and/or the subducting lithosphere on present-day plate motions. We are able to investigate the mutual role of mantle drag, plate interactions, and the subducting slab on the kinematics of the India and

Arabia collisional system and identify a deep mantle convective current as the major driver of convergence.

## 2. Methods

To examine the mantle drag contributions due to different buoyancy force distributions, we use 3-D, spherical mantle flow computations (Hager and O'Connell, 1981). To model mantle circulation, we solve the infinite Prandtl number, Stokes equation for incompressible fluid flow (Boussinesq approximation) in a global, spherical shell domain using the finite-element code CitcomS (Zhong et al., 2000), with our own modifications as shared through CG (geodynamics.org). We employ a numerical resolution of ~20 km laterally in the upper mantle which we tested was sufficient to resolve regional, viscous behavior of the lithosphere on the ~100 km scales we are interested in, while maintaining a globally consistent model (Faccenna and Becker, 2010). Our parameter choices as described subsequently are motivated by previous work on fitting plate motions and the geoid (e.g. Ghosh et al., 2010). The solution for the instantaneous mantle flow, indicative of present-day deformation, relies on assuming that density anomalies and viscosity are known within the computational domain. For Stokes flow and linear rheologies, velocities scale with density anomaly over viscosity, and stresses with density anomaly only, for first order.

The rheology of the mantle is assumed Newtonian viscous and most models only have radial viscosity variations besides weak zones which are confined to the lithosphere (down to 100 km depth), have 300 km width for most models, and a viscosity reduction to 0.01 of the lithospheric viscosity. Plate motions are partially controlled by the weak zone geometry which mainly follows the major plate boundaries (Fig. 2A). The intraplate weak zones in Asia are geologically motivated and focus deformation in India and a south-east corner of the Eurasian plate. Other choices for weak zone width (150 km) and geometry are explored in Fig. S6 (see Supplementary material). The reference, radial viscosity structure is  $5 \cdot 10^{22}$  Pas in the lithosphere,  $10^{21}$  Pas from 100 to 660 km, and  $5 \cdot 10^{22}$  Pas in the lower mantle. Fig. S4 shows results for models including lateral viscosity variations.

Mantle driving forces due to upwellings and downwellings in our models are mainly controlled by the assumed density structure. Density models may be constructed by scaling the velocity anomalies from seismic tomography to temperature (e.g. Hager et al., 1985), by inferring density for slabs alone, based on seismicity in Wadati-Benioff zones and/or inferred past subduction (e.g. Hager, 1984; Lithgow-Bertelloni and Richards, 1998; Ricard et al., 1993), or by mixed models that explore the respective role of slabs versus tomography and edge forces (e.g. Becker and O'Connell, 2001; Conrad and Lithgow-Bertelloni, 2002; Ghosh et al., 2010; Stadler et al., 2010). The reference density model is based on the composite S wave tomography SMEAN (Becker and Boschi, 2002). We remove velocity anomalies underneath cratonic keels (from 3SMAC by Nataf and Ricard, 1996) down to 250 km to avoid being affected by presumably compositional anomalies there (Forte, 2007). At a Rayleigh number of  $3.4 \cdot 10^8$  (definition of Zhong et al., 2000), non-dimensional temperatures are scaled such that density,  $\rho$ , anomalies go as  $d\ln\rho/d\lnV_S = 0.2$  for S wave tomography, and  $d\ln\rho/d\lnV_P = 0.4$  for P wave models, consistent with previous global circulation modeling (Becker and O'Connell, 2001).

We adopt such a scaling for simplicity, realizing that compositional anomalies and depth-dependent mineral physics relationships will complicate the mapping between velocity anomalies and density (e.g. Simmons et al., 2010; Steinberger and Calderwood, 2006). We assume that, by taking into account cratonic roots, all remaining anomalies in the upper mantle are of thermal nature for the reference model, but also tested a model without any negatively buoyant anomalies above 250 km underneath continents (Fig. S5A).

In addition to tomography-only density, we consider upper mantle models that are entirely or partially based on slab structure inferred from Wadati–Benioff zone seismicity, based on the RUM geometry (Gudmundsson and Sambridge, 1998), as in Ghosh et al. (2010), and models where only positive or negative velocity anomalies from tomography are used. No crustal density anomalies or other effects leading to crustal driving forces due to gravitational potential energy variations are considered.

Our approach to predict plate motions follows Ricard and Vigny (1989) and Zhong et al. (2000) and is described in detail elsewhere (Becker, 2006; Faccenna and Becker, 2010). It is geared toward

exploring complex collisional systems by allowing for different sets of surface boundary conditions, and by exploring the role of lithospheric weak zones in models that allow for lateral variations in viscosity (cf. King et al., 1992). Surface kinematic boundary conditions for most models are shear-stress free (i.e. the surface is free slip), allowing for dynamically-consistent plate motions. Results are presented for a regional zoom-in of the global models around the Tethyan, with all velocities rotated into a Eurasia-fixed reference frame. The corresponding, best-fit Euler pole is obtained from the surface velocities within that plate, allowing for any potential intra-plate deformation. We also run models to test the influence of single

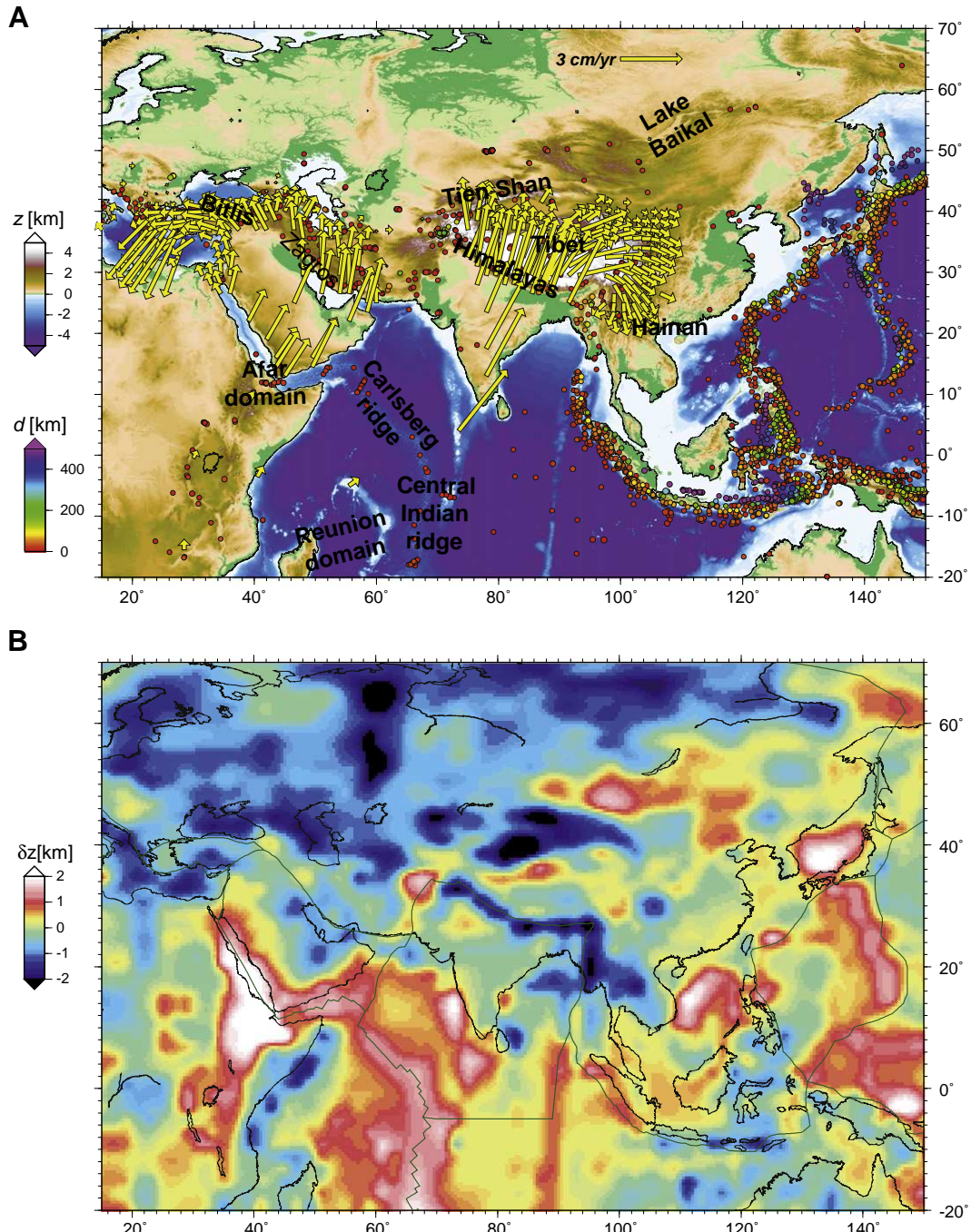


**Fig. 1.** Topography and deformation indicators for the Tethyan belt. A) Geodetic velocity field (Zhang et al., 2004; Gan et al., 2007; ArRajehi et al., 2010), topography ( $z$ ), and seismicity (Engdahl et al., 1998) colored by depth ( $d$ ), with major geographic features labeled. B) Residual topography,  $\delta z$ , relative to a regional mean, estimated by correcting for crustal isostatic adjustment (see Supplementary material). (For interpretation of the references to color in this figure legend, the reader is referred to the web version of this article.)

or overall plate motions on the kinematics of the colliding system by prescribing velocities on part of the surface, while leaving the rest shear-stress free, as in Faccenna and Becker (2010).

The normal stresses generated by viscous flow at the surface are used to infer the instantaneous surface deflection that would be expected due to convection ("dynamic topography") (Ricard et al., 1984; Richards and Hager, 1984). Assuming that all non-crustal topography is due to active flow, this signal can be compared to observed topography once the effect of crustal isostatic adjustment is removed to arrive at "residual topography" (Fig. 1B) (e.g. Daradich et al., 2003; Gurnis et al., 2000). Model results are evaluated in the light of the present-day geodetic velocity fields and geomorphological information concerning the vertical motion.

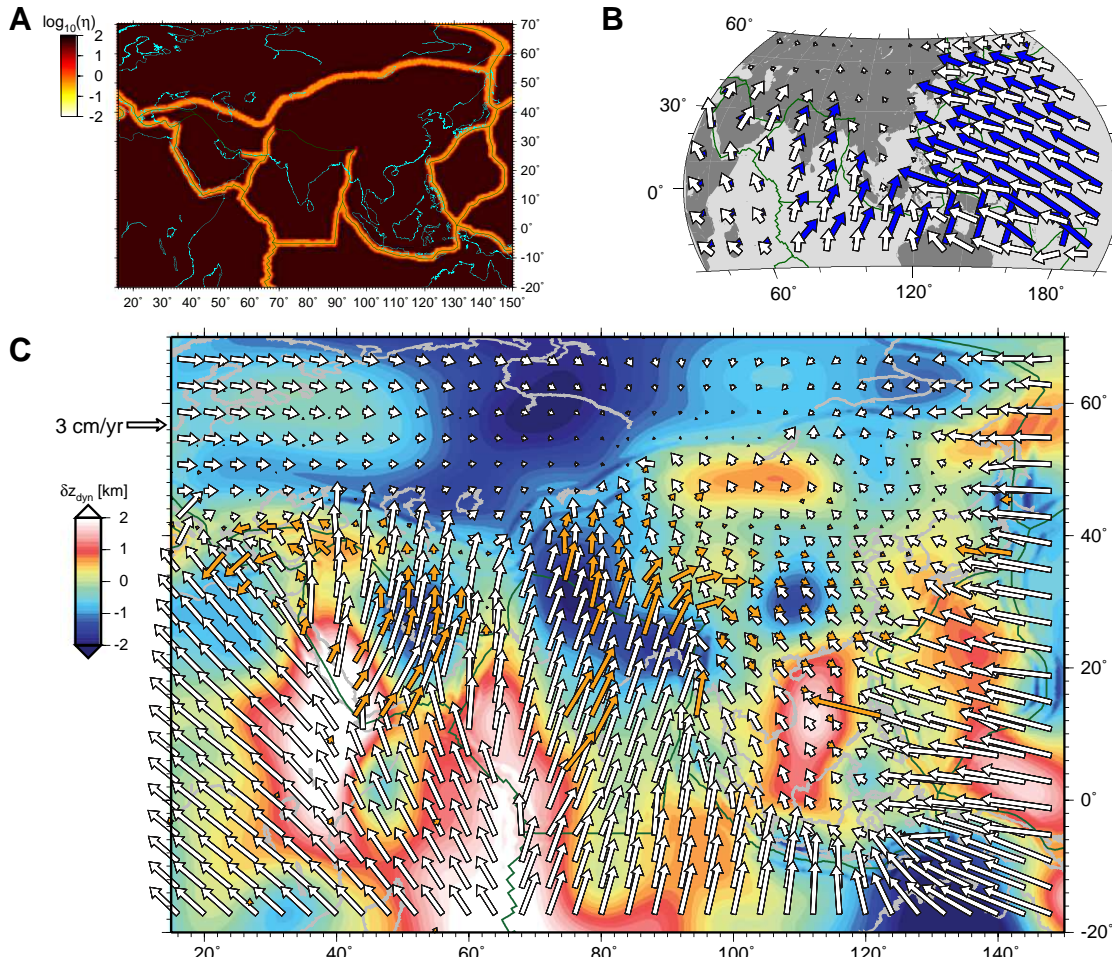
### 3. Results

Fig. 2 shows surface velocities for our reference model. The motion of the Indian plate (Fig. 2C) is fairly well reproduced compared to geodetic velocities (orange arrows, averaged from Fig. 1A). The direction of the motion of Arabia is also matched, although its rate is overestimated. Velocities for the Pacific and Philippine Sea plate are roughly fit by the model, with an under-predicted rate. The motion of the Australian plate, conversely, is not correctly reproduced, but as shown next, this is not significantly affecting the kinematics of

the colliding system. We therefore refrain from optimizing our models for global motion fit (cf. Forte, 2007), for simplicity. We also do not optimize the location or properties of the weak zones. However, Fig. S6B shows results when an alternative plate boundary geometry is used instead; motions are overall consistent with those shown in Fig. 2C.

In detail, the motion of India shows a progressive decrease in velocity moving from the Carlsberg ridge to the collisional zone (Fig. 2C). This is seen in sections across the Indian and Arabian plates, showing an upwelling in the upper and lower mantle (Fig. 3A and B), pushing plates toward the collisional zone, where a high velocity anomaly – a trace of an older subduction zone – (Fig. 3C and D) represents the sinking component of the return flow into the upper and lower mantle. Vertical mass transport rates for slab sinkers are predicted to be typically  $\sim 1.5 \text{ cm/yr}$  at  $\sim 660 \text{ km}$  and in the lower mantle, broadly consistent with geological-tomographic reconstructions (van der Meer et al., 2010).

Overall, the upwelling-downwelling circuit forms a convection cell ("conveyor belt," realizing that there is three-dimensionality to the flow not seen in 2D cells, Fig. 4). This circulation encompasses the motion of the India plate, with northward flow concentrated in the upper mantle and the south-directed return flow in the lower mantle. The low velocity anomalies associated with this flow are found beneath Ethiopia-Afar, spreading northward toward Arabia



**Fig. 2.** Reference flow model for the Tethyan belt, part I. The density structure used for the computations is based on SMEAN tomography (Becker and Boschi, 2002), with anomalies in cratonic regions (from Nataf and Ricard, 1996) in the upper 250 km removed. A) Plate boundaries are treated as weak narrow belts, as depicted by the  $\log_{10}$  of surface viscosity relative to the reference of  $10^{21} \text{ Pas}$ . B) Large-scale comparison between predicted (white) and observed (NUVEL-1A model, blue (DeMets et al., 1994)) velocities. C) Predicted surface velocities (white vectors), geodetic velocities (orange, averaged from Fig. 1A), and "dynamic topography,"  $\delta z_{\text{dyn}}$  (i.e. instantaneous surface deflection due to mantle flow) of the Tethyan plate system. NUVEL-1A plate boundaries are shown in green. All velocities are shown in a (best-fit) Eurasia fixed reference frame. See Fig. 3 for deep mantle flow. (For interpretation of the references to color in this figure legend, the reader is referred to the web version of this article.)

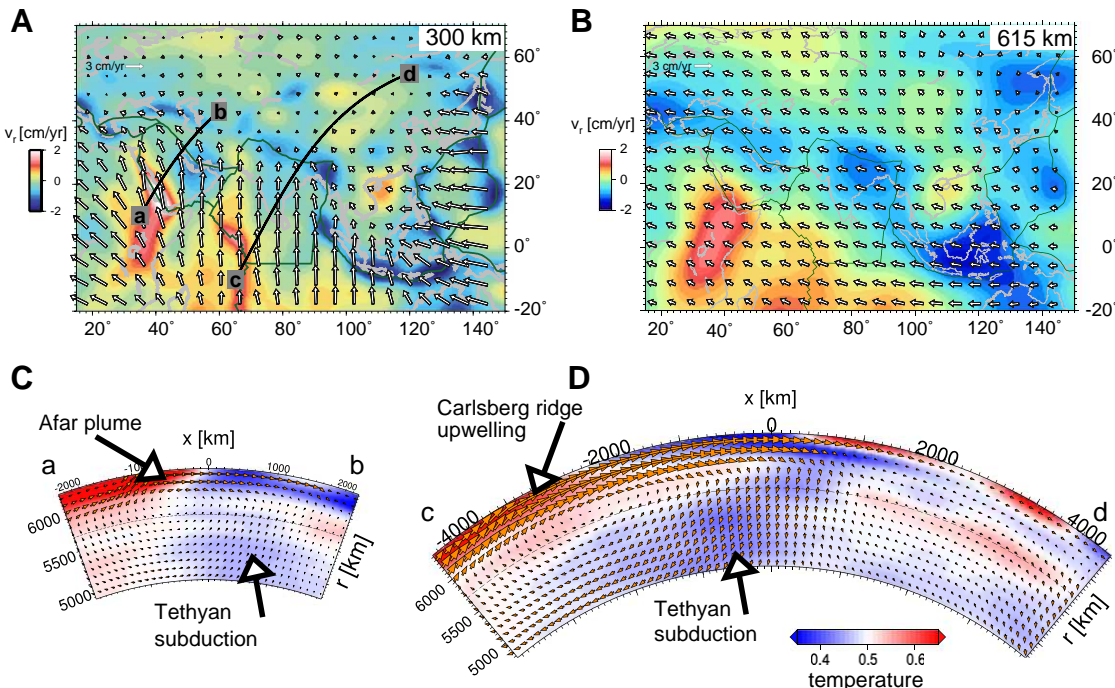


**Fig. 3.** Reference flow model for the Tethyan belt, part II. Horizontal (white vectors) and vertical flow (background shading) field at 300 km (A) and 615 km (B) depth, in a Eurasia fixed reference frame. C) and D): Cross-sections from Afar to Iran, and from the Carlsberg ridge to Central Asia, respectively (trace of cross section marked in A), with non-dimensional temperature in the background. Compare Fig. 2 for surface-near model properties. (For interpretation of the references to color in this figure legend, the reader is referred to the web version of this article.)

and beneath Réunion trending northward beneath the Carlsberg ridge (Fig. 3). The convective pattern associated with the conveyor belt produces a multi-scale topographic signal that, to first order, visually matches many features of the residual topography (cf. Figs. 1B and 2C). This indicates that at least part of the topography of the Tethyan and surrounding regions may be dynamically supported by the mantle. A previously recognized example is the prominent positive topography over east Africa-eastern Arabia, producing an overall tilting of the Arabian plate (Daradich et al., 2003), already attributed to the large scale low-velocity mantle anomaly mapped under Africa (Gurnis et al., 2000; Lithgow-Bertelloni and Silver, 1998). This large-scale topographic signal is rooted toward the south, on what is presumably a hotspot acting over the last 30 Ma, first over east Africa and presently beneath Afar. Our model matches the residual topography estimate (Fig. 1B), showing a broad upwelling extending north toward the Middle East (cf. Boschi et al., 2010).

Positive surface deflections inferred from mantle flow also extend over the presently active hotspot beneath Réunion, the origin of the Deccan trap eruption at the end of the Cretaceous. This feature extends northward along the Carlsberg and Central Indian Ridges and also connects to the south-Africa lower mantle, low velocity anomaly (Gurnis et al., 2000; Steinberger et al., 2001). In our model, this upwelling is responsible for a large part of the driving force of the India motion. Other high dynamic topography features are found in the north China Sea and in the Baikal region. The Hainan volcano is found over a broad upwelling zone in south China which has been related to plumes forming on top of a prominent low-velocity anomaly in the mantle (Lebedev and Nolet, 2003; Lei et al., 2009). Doming, volcanism and uplift beneath the Baikal-Mongolia plateau have also been associated with lithosphere plume interactions (Windley and Allen, 1993). The Tethyan belt itself is only locally (Caucasus-Anatolia-Iran) marked by a positive topography signal. Comparison with the residual topography map shows that most of the elevation is compensated by crustal thickening, predicting small, if any, dynamic uplift in the Tibetan plateau for this particular model.

### 3.1. Sensitivity tests

To further explore the contribution of mantle flow on the regional plate motions, we start from the reference model, and set to zero the motion of all plates outside the Eurasian/Arabian domain (Fig. 5A). This model shows that the influence of the surrounding plate motions is to turn the velocity field northerly for India and Arabia by  $\sim 10^{\circ}$ – $20^{\circ}$ , but velocity amplitudes are not affected significantly. Prescribing the plate motion of Australia or Africa (Fig. 5B and C) to conform to NUVEL-1A (DeMets et al., 1994) also does not produce significant deviations from our reference model (compare Fig. 5C and D with Fig. 2C). This implies that plate interactions produce only a moderate influence on the orientation of the colliding motion, indicating the primary role of driving mantle tractions associated with the conveyor belt.

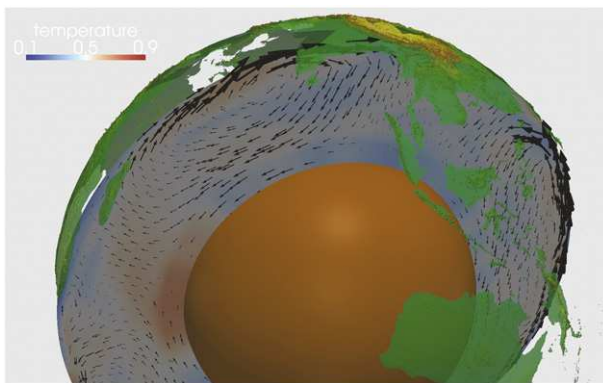


**Fig. 4.** Three-dimensional view of the conveyor belt beneath India obtained by visualizing a cross-section of the reference model shown in Figs. 2 and 3. (For interpretation of the references to color in this figure legend, the reader is referred to the web version of this article.)

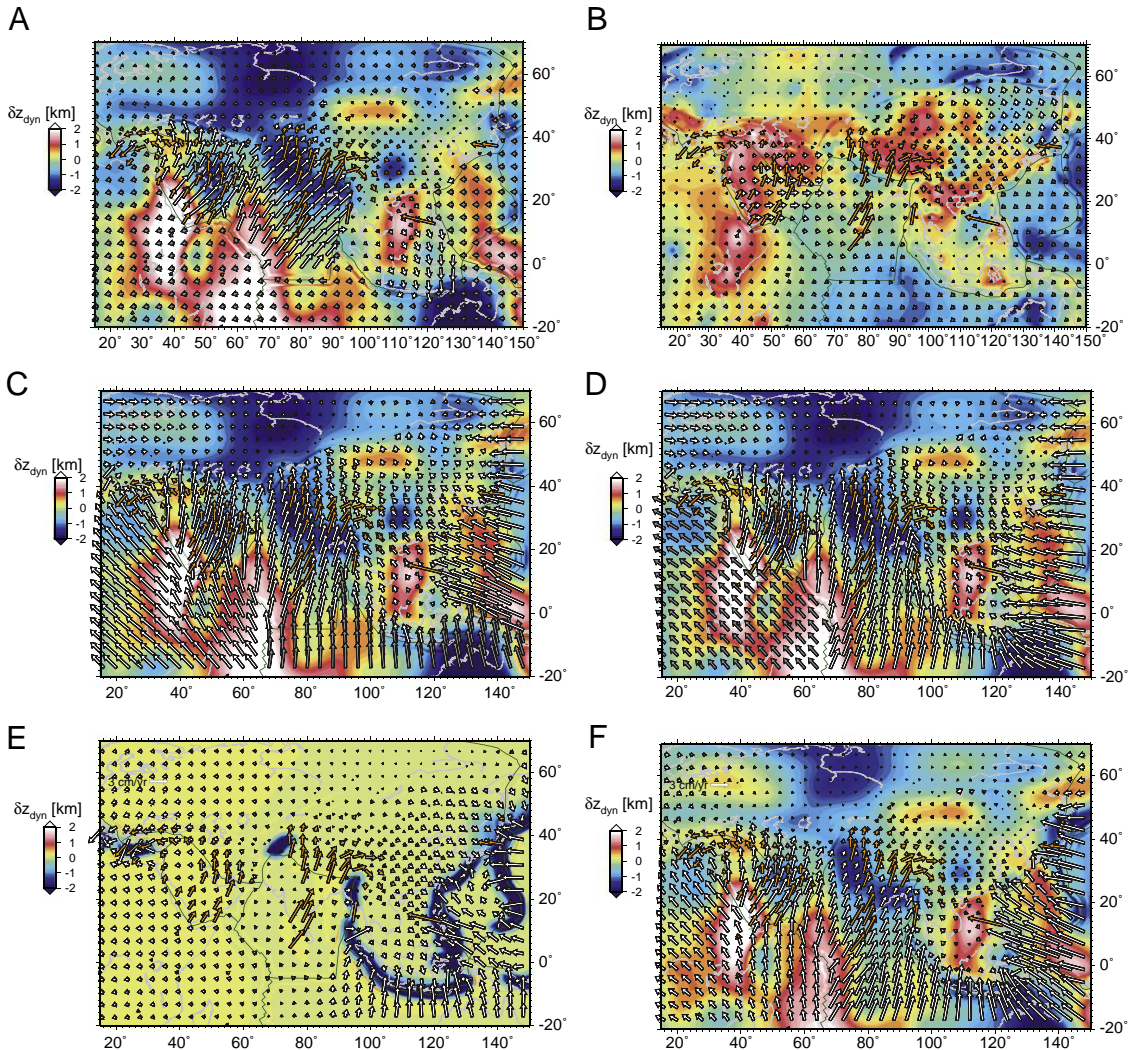


**Fig. 5.** Additional flow models for the Tethyan belt. Surface velocities and dynamic topography, as in Fig. 2C. A) Flow generated by density anomalies only, holding the surface motions fixed to zero outside India and Arabia, for the reference model of Fig. 2; B) Flow generated by density anomalies only (i.e. surface held fixed outside the India and Arabia) based on MIT08 P wave tomography (Li et al., 2008b); C) Flow generated by density anomalies holding the Australian plate moving at NUVEL-1A model rates (DeMets et al., 1994); D) Flow generated by density anomalies holding the African plate moving at NUVEL-1A rates; E) Flow generated by density anomalies restricted within the Wadati Benioff zones; F) Flow generated by density anomalies from reference models, including the first 100 km, but with upper mantle negative density anomalies restricted to Wadati Benioff zones and slow tomographic velocities only between 100 and 660 km. (For interpretation of the references to color in this figure legend, the reader is referred to the web version of this article.)

The individual roles of upwellings and downwellings can be inferred by comparing our reference model, which is based on SMEAN, with one where density is scaled from recent *P*-wave tomography (Li et al., 2008b) (MIT08). By virtue of the construction with its reliance on body waves and the specific data sets, the MIT *P* model has superior resolution close to slabs, and underneath parts of Asia (Li et al., 2008b). The high velocity zone in the shallow layer in the SMEAN model covers a large part of the collisional zone, whereas in MIT08 it is restricted to the subduction zones (Fig. S1). More importantly, the MIT08 model does not show the low velocity anomaly beneath Réunion and the Carlsberg ridge, presumably because of lack of coverage (SMEAN includes information from surface waves). As a result, India is not moving correctly (Figs. 5B and S2).

While any convective cell consists of both upwellings and downwellings, by definition (Fig. 4), one may wish to isolate the importance of relatively focused, active plumes or slab sinkers. One approach is to zero out either slow ("hot") or fast ("cold") anomalies from the tomographic model and compute the respective flow (see Supplementary material). Since relative, rather than absolute, density anomalies are driving mantle flow, such tests cannot

straightforwardly isolate individual mantle components. However, results (Figs. S5B and C) imply that broad-scale upwellings and downwellings are the largest drivers of the conveyor belt, and localized upwellings such as underneath the Carlsberg ridge and Afar contribute a significant component.

The role of upper mantle slabs in driving plate motions can be tested by assigning density anomalies to regions with Wadati-Benioff seismicity. In our study region, deep seismicity is distributed along the Pacific margins, along Java-Sumatra-Burma, beneath the Hindu Kush cluster, and, far to the west, along the Hellenic trench (Fig. 1A). The flow predictions for slabs only (in the Gudmundsson and Sambridge, (1998) locations, Fig. 5E) indicate that subduction does drive Australia northward, although at a significantly reduced rate. India and Arabia move slowly, if at all, with Arabia-Anatolia mainly pulled to the west by the Hellenic slab. The northward motion of India and Arabia increases by adding lower mantle anomalies and, even more, by adding upper mantle slow velocity anomalies (Fig. 5F). In addition, this latter model shows a good fit with crustal velocities. We take this to indicate the role of active subduction zones on the side of the colliding system, which leads to an

important regional modification of the overall convergence kinematics that are themselves mainly driven by a large-scale mantle upwelling. This is particularly evident on the Mediterranean side, where the Hellenic slab is pulling Anatolia westward (cf. Boschi et al., 2010).

#### 4. Discussion

Given our results, we can now infer the most important driving forces for the Tethyan collisional system at present-day. The pull exerted by subducting lithosphere is modeled by density anomalies either restricted to the high velocity regions in the upper mantle as imaged by tomography, or to Wadati Benioff zones. Models with well resolved high velocity anomalies in the subduction zone, but poorly resolved low velocity anomalies in upper mantle regions, such as underneath the Carlsberg ridge, produce no motion of India (Figs. 5A and S2). Similarly, given that Wadati–Benioff seismicity is almost absent beneath the collision area, the restriction of the density anomaly to the seismically active slabs, expectedly, does not lead to any significant motion of the colliding plates.

While the lack of a direct link between slab-related driving forces and India and Arabia plate motions in our models is not entirely representative of all aspects of the slab pull mechanism, we infer that the role of upper mantle slabs on the present-day velocity field cannot be dominant. Geological evidence indicates that the Himalayan orogeny has been punctuated by episodes of slab rupture, the first probably occurring soon after collision (Chemenda et al., 2000; Replumaz et al., 2010). This is similar to what has been proposed for Arabia (Faccenna et al., 2006; Hafkenscheid et al., 2006), and would limit the possible action of slab-pull forces. Recent tomographic images illustrate that the slabs beneath India and Arabia (e.g. Keskin, 2003; Li et al., 2008b) are now rather small, perhaps underthrusting sub-horizontally. Shallow slab segments appear separated from deeper slabs, which are either ponding above the 660 km phase transition, or in the lower mantle behind the present-day subduction zone (Hafkenscheid et al., 2006; van der Voo et al., 1999).

The gravitational potential energy forces related to lithospheric thickening and continental structure are here not taken into account directly (cf. Copley et al., 2010). However, including the shallowest 100 km velocity anomalies from tomography means including most of the half-space cooling signature of oceanic lithosphere and hence ridge push (Fig. 5F). A comparison with a model without that layer (not shown) indicates that this contribution is, however, not dominant. Ghosh et al. (2006) estimate the contribution of ridge push in the Indian ocean and conclude that the gravitational potential energy exerted by the Tibetan plateau ( $\sim 3 \cdot 10^{12}$  N/m) exceeds the ridge push level. Consistent with our findings, Ghosh et al. (2006) also point out that an additional force, presumably mantle drag, is required to fit the present-day stress field of the region. For the case of Arabia, in addition, the ridge push contribution cannot be large because the Gulf of Aden–Red Sea is only a narrow, incipient ocean. In terms of plate interactions, the contribution of the northward advancing Australian plate is relevant in determining the direction of motion of India, but appears to not affect the amplitudes of India motion strongly. This is shown by comparing our reference model with one where Australian motion is prescribed (Figs. 2C and 5C).

This leads us to suggest that the most important force contribution is related to deep-rooted mantle flow. The reference model (Figs. 2 and 3) and a range of tests for different tomographic models and rheology (including Figs. 5, S3, S4), consistently show that an important contribution for plate motion in the system is derived from the large-scale conveyor belt beneath the two colliding plates (Fig. 4). In particular, the comparison between different tomography models, and positive or negative anomaly components (Figs. 5 and S5) shows that an active upwelling beneath

the Réunion–Carlsberg is, and probably has been, a fundamental ingredient for the collisional history of India. These findings are in some contrast to the global models of (Steiner and Conrad, 2007) who concluded that active upwellings degraded the fit to global plate motions compared to slab-only models (cf. Becker and O'Connell, 2001; Conrad and Lithgow-Bertelloni, 2002).

Comparing the reference model with Fig. 5F shows that incorporating the density distribution within upper mantle subduction zones in addition to active upwellings gives a better match to the overall velocity field. For example, incorporating the density anomaly within the Hellenic trench promotes the westward motion of Anatolia. However, all of our main models fail to reproduce the toroidal flow trajectories that are pronounced on the eastern side of the India indenter, where motions turn to SE orientations with respect to Eurasia. We deduce that this flow component may be related to lower crustal, or decoupled lithospheric, flow underneath the Yunnan domain as suggested by (Royden et al., 1997). Material appears to escape laterally from the convergence zone under the gravitational potential energy of the high plateau with respect to the surrounding lowlands (cf. Royden, 2008). This motion is perhaps assisted by uppermost mantle upwellings (Fig. 5A) or slab suction (Fig. 5E), but these effects are swamped in our models by the overall convergent flow, and rheologically more complex models with regional decoupling may be required (Clark et al., 2005; Flesch et al., 2005; Sol et al., 2007).

#### 5. Conclusions

We substantiate previous suggestions that mantle drag and active upwellings are highly efficient in driving continental plates (Alvarez, 2010; Cande and Stegman, 2011; Gurnis and Torsvik, 1994; van Hinsbergen et al., 2011). Our models indicate that a plume-associated “conveyor belt” represents the primary mechanism for India and Arabia to collide, indenting against the Eurasian plate and supporting the thick Tibetan and Iranian mountain ranges. We suggest that particularly the active upwelling component of the conveyor belt is a significant driving force. Over the geological history of the collision, it might have played a sustained role in breaking continental plates into small pieces and pushing them away against the upper plate. The present-day upwelling extends from East Africa to the Indian Ocean, and represents the shallow, upper mantle expression of the deep south African low-velocity zone. Our models suggest that the gravitational pull induced by subduction represents a secondary mechanism, accommodating convergence and leaving behind drips of high velocity material in the mantle beneath the advancing collisional zone.

#### Acknowledgments

We thank our reviewers J. van Hunen and J.J.D. van Hinsbergen for detailed and insightful comments that helped clarify the presentation, A. Ghosh for assistance with density models, CitcomS authors including L Moresi, S. Zhong, E. Tan, and A. McNamara for their contributions, CIG (geodynamics.org), and seismologists who share their tomographic models in electronic form. Computations were performed on USC's High Performance Computing Center, and research was supported by NSF grants EAR 0930046 and 0643365. C.F. was supported by TOPOEUROPE.

#### Appendix A. Supplementary data

Supplementary data to this article can be found online at doi:10.1016/j.epsl.2011.08.021.

## References

- Allen, M.B., Armstrong, H.A., 2008. Arabia–Eurasia collision and the forcing of mid-Cenozoic global cooling. *Paleogeogr. Paleoclimatol. Palaeoecol.* 265, 3152–3158.
- Alvarez, W., 1990. Geologic evidence for the plate-driving mechanism: the continental undertow hypothesis and the Australian–Antarctic discordance. *Tectonics* 9, 1213–1220.
- Alvarez, W., 2010. Protracted continental collisions argue for continental plates driven by basal traction. *Earth Planet. Sci. Lett.* 296, 434–442.
- ArRajehi, A., McClusky, S., Reilinger, R., Daoud, M., Alchalbi, A., Ergintav, S., Gomez, F., Sholan, J., Bou-Rabee, F., Ougubazghi, G., Haileab, B., Fisseha, S., Asfaw, L., Mahmoud, S., Rayan, A., Bendik, R., Kogan, L., 2010. Geodetic constraints on present day motion of the Arabian Plate: implications for Red Sea and Gulf of Aden rifting. *Tectonics* 29, TC3011. doi:[10.1029/2009TC002482](https://doi.org/10.1029/2009TC002482).
- Becker, T.W., 2006. On the effect of temperature and strain-rate dependent viscosity on global mantle flow, net rotation, and plate-driving forces. *Geophys. J. Int.* 167, 943–957.
- Becker, T.W., Boschi, L., 2002. A comparison of tomographic and geodynamic mantle models. *Geochem. Geophys. Geosyst.* 3, 1. doi:[10.1029/2001GC000168](https://doi.org/10.1029/2001GC000168).
- Becker, T.W., O’Connell, R.J., 2001. Predicting plate velocities with geodynamic models. *Geochem. Geophys. Geosyst.* 2, 12. doi:[10.1029/2001GC000171](https://doi.org/10.1029/2001GC000171).
- Bellahsen, N., Faccenna, C., R., F.J.M., D., Jolivet, L., 2003. Why did Africa separate from Africa? Insight from 3D laboratory experiments. *Earth Planet. Sci. Lett.* 216, 365–381.
- Boschi, L., Faccenna, C., Becker, T.W., 2010. Mantle structure and dynamic topography in the Mediterranean Basin. *Geophys. Res. Lett.* 37, L20303. doi:[10.1029/2010GL045001](https://doi.org/10.1029/2010GL045001).
- Cande, S.C., Stegman, D.R., 2011. Indian and African plate motions driven by the push force of the Réunion plume head. *Nature* 475, 47–52.
- Cande, S.C., Patriat, P., Dyment, J., 2010. Motion between the Indian, Antarctic and African plates in the early Cenozoic. *Geophys. J. Int.* 183, 127–149.
- Capitanio, F.A., Morra, G., Goes, S., Weinberg, R.F., Moresi, L., 2010. India–Asia convergence driven by the subduction of the Greater Indian continent. *Nat. Geosci.* 3, 136–139.
- Chemenda, A.I., Burg, J.P., Mattauer, M., 2000. Evolutionary model of the Himalaya–Tibet system: geopoem based on new modelling, geological and geophysical data. *Earth Planet. Sci. Lett.* 174, 397–409.
- Clark, M.K., Bush, J.W.M., Royden, L.H., 2005. Dynamic topography produced by lower crustal flow against rheological strength heterogeneities bordering the Tibetan Plateau. *Geophys. J. Int.* 162, 575–590.
- Cloetingh, S., Wortel, M.J.R., 1986. Stress in the Indo–Australian plate. *Tectonophysics* 132, 49–67.
- Cloos, M.N., 1993. Lithospheric buoyancy and collisional orogenesis: subduction of oceanic plateaus, continental margins, island arcs, spreading ridges and seamounts. *Geol. Soc. Am. Bull.* 105, 715–737.
- Coblenz, D.D., Zhou, S., Hillis, R.R., Richardson, R.M., Sandiford, M., 1998. Topography, boundary forces, and the Indo–Australian intraplate stress field. *J. Geophys. Res.* 103, 919–931.
- Conrad, C.P., Lithgow-Bertelloni, C., 2002. How mantle slabs drive plate tectonics. *Science* 298, 207–209.
- Copley, A., Avouac, J.-P., Royer, J.-Y., 2010. India–Asia collision and the Cenozoic slowdown of the Indian plate: implications for the forces driving plate motions. *J. Geophys. Res.* 115, B03410. doi:[10.1029/2009JB006634](https://doi.org/10.1029/2009JB006634).
- Daradich, A., Mitrovica, J.X., Pysklywec, R.N., Willet, S.D., Forte, A., 2003. Mantle flow, dynamic topography, and rift-flank uplift of Arabia. *Geology* 31, 901–904.
- DeMets, C., Gordon, R.G., Argus, D.F., Stein, S., 1994. Effect of recent revisions to the geomagnetic reversal time scale on estimates of current plate motions. *Geophys. Res. Lett.* 21, 2191–2194.
- Ebbing, C.J., Sleep, N.H., 1998. Cenozoic magmatism throughout east Africa resulting from impact of a single plume. *Nature* 395, 788–791.
- Engdahl, E.R., van der Hilst, R.D., Buland, R., 1998. Global teleseismic earthquake relocation with improved travel times and procedures for depth determination. *Bull. Seismol. Soc. Am.* 88, 722–743.
- Faccenna, C., Becker, T.W., 2010. Shaping mobile belts by small-scale convection. *Nature* 465, 602–605.
- Faccenna, C., Bellier, O., Martinod, J., Piromallo, C., Regard, V., 2006. Slab detachment beneath eastern Anatolia: a possible cause for the formation of the North Anatolian fault. *Earth Planet. Sci. Lett.* 242, 85–97.
- Flesch, L.M., Holt, E.E., Silver, P.G., Stephenson, M., Wang, C.-Y., Chan, W.W., 2005. Constraining the extent of crustmantle coupling in central Asia using GPS, geologic, and shear wave splitting data. *Earth Planet. Sci. Lett.* 238, 248–268.
- Forte, A.M., 2007. Constraints on seismic models from other disciplines—implications for mantle dynamics and composition. In: Schubert, G., Bercovici, D. (Eds.), *Treatise on Geophysics*. Elsevier, Amsterdam, pp. 805–858.
- Gaina, C., Müller, R., Brown, B., Ishihara, T., Ivanov, S., 2007. Breakup and early seafloor spreading between India and Antarctica. *Geophys. J. Int.* 170, 151–170.
- Gan, W., Zhang, P., Shen, Z., Niu, Z., Wang, M., Wan, Y., Zhou, D., Cheng, J., 2007. Present day crustal motion within the Tibetan Plateau inferred from GPS measurements. *J. Geophys. Res.* 113, B08416. doi:[10.1029/2005JB004120](https://doi.org/10.1029/2005JB004120).
- Ghosh, A., Holt, W.E., Flesch, L.M., Haines, A.J., 2006. Gravitational potential energy of the Tibetan Plateau and the forces driving the Indian plate. *Geology* 34, 321–324.
- Ghosh, A., Becker, T.W., Zhong, S., 2010. Effects of lateral viscosity variations on the geoid. *Geophys. Res. Lett.* 37, L01301. doi:[10.1029/2009GL040426](https://doi.org/10.1029/2009GL040426).
- Gudmundsson, O., Cambridge, M., 1998. A regionalized upper mantle (RUM) seismic model. *J. Geophys. Res.* 103, 7121–7136.
- Guillot, S., Garzanti, E., Baratoux, D., Marquer, D., Mahéo, G., de Sigoyer, J., 2003. Reconstructing the total shortening history of the NW Himalaya. *Geochem. Geophys. Geosyst.* 4, 7. doi:[10.1029/2002GC000484](https://doi.org/10.1029/2002GC000484).
- Gurnis, M., Torsvik, T., 1994. Rapid drift of large continents during the Late Precambrian and Paleozoic: paleomagnetic constraints and dynamics models. *Geology* 22, 1023–1026.
- Gurnis, M., Mitrovica, J.X., Ritsema, J., van Heijst, H.-J., 2000. Constraining mantle density structure using geological evidence of surface uplift rates: the case of the African superplume. *Geochem. Geophys. Geosyst.* 1. doi:[10.1029/1999GC000035](https://doi.org/10.1029/1999GC000035).
- Hafkenscheid, E., Wortel, M.J.R., Spakman, W., 2006. Subduction history of the Tethyan region derived from seismic tomography and tectonic reconstructions. *J. Geophys. Res.* 111, B08401. doi:[10.1029/2005JB003791](https://doi.org/10.1029/2005JB003791).
- Hager, B.H., 1984. Subducted slabs and the geoid: constraints on mantle rheology and flow. *J. Geophys. Res.* 89, 6003–6015.
- Hager, B.H., O’Connell, R.J., 1981. A simple global model of plate dynamics and mantle convection. *J. Geophys. Res.* 86, 4843–4867.
- Hager, B.H., Clayton, R.W., Richards, M.A., Comer, R.P., Dziewoński, A.M., 1985. Lower mantle heterogeneity, dynamic topography and the geoid. *Nature* 313, 541–545.
- Hatzfeld, D., Molnar, P., 2010. Comparisons of the kinematics and deep structures of the Zagros and Himalaya and of the Iranian and Tibetan plateaus and geodynamic implications. *Rev. Geophys.* 48, RG2005. doi:[10.1029/2009RG000304](https://doi.org/10.1029/2009RG000304).
- Johnson, M.R.W., 2002. Shortening budgets and the role of continental subduction during the India–Asia collision. *Earth Sci. Rev.* 59, 101–123.
- Jolivet, L., Faccenna, C., 2000. Mediterranean extension and the Africa–Eurasia collision. *Tectonics* 6, 1095–1107.
- Keskin, M., 2003. Magma generation by slab steepening and breakoff beneath a subduction–accretion complex: an alternative model for collision-related volcanism in eastern Anatolia, Turkey. *Geophys. Res. Lett.* 30, 8046. doi:[10.1029/2003GL018019](https://doi.org/10.1029/2003GL018019).
- King, S.D., Gable, C.W., Weinstein, S.A., 1992. Models of convection-driven tectonic plates: a comparison of methods and results. *Geophys. J. Int.* 109, 481–487.
- Lebedev, S., Nolet, G., 2003. Upper mantle beneath Southeast Asia from S velocity tomography. *J. Geophys. Res.* 108, 2048. doi:[10.1029/2000JB000073](https://doi.org/10.1029/2000JB000073).
- Lei, J., Zhao, D., Steinberger, B., Wu, B., Shen, F., Li, Z., 2009. New seismic constraints on the upper mantle structure of the Hainan plume. *Phys. Earth Planet. Inter.* 33–50.
- Li, C., van der Hilst, R.D., Meltzer, A.S., Engdahl, E.R., 2008a. Subduction of the Indian lithosphere beneath the Tibetan Plateau and Burma. *Earth Planet. Sci. Lett.* 274, 157–168.
- Li, C., van der Hilst, R.D., Engdahl, E.R., Burdick, S., 2008b. A new global model for P wave speed variations in Earth’s mantle. *Geochem. Geophys. Geosyst.* 9, Q05018. doi:[10.1029/2007CC001806](https://doi.org/10.1029/2007CC001806).
- Lithgow-Bertelloni, C., Richards, M.A., 1998. The dynamics of Cenozoic and Mesozoic plate motions. *Rev. Geophys.* 36, 27–78.
- Lithgow-Bertelloni, C., Silver, P.G., 1998. Dynamic topography, plate driving forces and the African superswell. *Nature* 395, 269–272.
- McClusky, S., Reilinger, R., Mahmoud, S., Sari, D.B., Tealeb, A., 2003. GPS constraints on Africa (Nubia) and Arabia plate motions. *Geophys. J. Int.* 155, 126–138.
- McQuarrie, N., Stock, J.M., Verdel, C., Wernicke, B.P., 2003. Cenozoic evolution of Neotethys and implications for the causes of plate motions. *Geophys. Res. Lett.* 30, 2036. doi:[10.1029/2003GL017992](https://doi.org/10.1029/2003GL017992).
- Meijer, P.T., Wortel, M.J.R., 1999. Cenozoic dynamics of the African plate with emphasis on the Africa–Eurasia collision. *J. Geophys. Res.* 104, 7405–7418.
- Molnar, P., Tapponnier, P., 1975. Cenozoic tectonics of Asia: effects of a continental collision. *Science* 189, 419–426.
- Nataf, H.-C., Ricard, Y., 1996. 3SMAC: an *a priori* tomographic model of the upper mantle based on geophysical modeling. *Phys. Earth Planet. Inter.* 95, 101–122.
- Patriat, P., Achache, J., 1984. India–Eurasia collision chronology has implications for crustal shortening and driving mechanism of plates. *Nature* 311, 615–621.
- Replumaz, A., Negredo, A., Guillot, S., Villaseñor, A., 2010. Multiple episodes of continental subduction during India/Asia convergence: insight from seismic tomography and tectonic reconstruction. *Tectonophysics* 483, 125–134.
- Ricard, Y., Vigny, C., 1989. Mantle dynamics with induced plate tectonics. *J. Geophys. Res.* 94, 17 543–17,559.
- Ricard, Y., Fleitout, L., Froidveaux, C., 1984. Geoid heights and lithospheric stresses for a dynamic Earth. *Ann. Geophys.* 2, 267–286.
- Ricard, Y., Richards, M.A., Lithgow-Bertelloni, C., Le Stunff, Y., 1993. A geodynamic model of mantle density heterogeneity. *J. Geophys. Res.* 98, 21 895–21,909.
- Richards, M., Hager, B.H., 1984. Geoid anomalies in a dynamic Earth. *J. Geophys. Res.* 89, 5987–6002.
- Royden, L.H., 2008. The geological evolution of the Tibetan Plateau. *Science* 321, 1054–1058.
- Royden, L.H., Burchfiel, B.C., King, B.C., Wang, E., Chen, Z., Shen, F., Liu, Y., 1997. Surface deformation and lower crustal flow in eastern Tibet. *Science* 276, 788–790.
- Simmons, N.A., Forte, A.M., Boschi, L., Grand, S.P., 2010. GyPSuM: a joint tomographic model of mantle density and seismic wave speeds. *J. Geophys. Res.* 115, B12310. doi:[10.1029/2010JB007631](https://doi.org/10.1029/2010JB007631).
- Sol, S., Meltzer, A., Bürgmann, R., van der Hilst, R.D., Chen, Z., Koons, P.O., Lev, E., Liu, Y.P., Zeitler, P.K., Zhang, X., Zhang, J., Zurek, B., 2007. Geodynamics of the southeastern Tibetan plateau from seismic anisotropy and geodesy. *Geology* 35, 563–566.

- Stadler, G., Gurnis, M., Burstedde, C., Wilcox, L.C., Alisic, L., Ghattas, O., 2010. The dynamics of plate tectonics and mantle flow: from local to global scales. *Science* 329, 1033–1038.
- Steinberger, B., Calderwood, A., 2006. Models of large-scale viscous flow in the earth's mantle with constraints from mineral physics and surface observations. *Geophys. J. Int.* 167, 1461–1481.
- Steinberger, B., Schmeling, H., Marquart, G., 2001. Large-scale lithospheric stress field and topography induced by global mantle circulation. *Earth Planet. Sci. Lett.* 186, 75–91.
- Steiner, S.A., Conrad, C.P., 2007. Does active mantle upwelling help drive plate motions? *Phys. Earth Planet. Inter.* 161, 103–114.
- Torsvik, T.H., Tucker, R.D., Ashwal, L.D., Carter, L.M., Jamtveit, B., Vidyadharan, K.T., Venkataramana, P., 2000. Late Cretaceous India–Madagascar fit and timing of break-up related magmatism. *Terra Nova* 13, 220–224.
- van der Meer, D.G., Spakman, W., van Hinsbergen, D.J.J., Amaru, M.L., Torsvik, T.H., 2010. Towards absolute plate motions constrained by lower-mantle slab remnants. *Nature Geo.* 3, 36–40.
- van der Voo, R., Spakman, W., Bijwaard, H., 1999. Tethyan subducted slabs under India. *Earth Planet. Sci. Lett.* 171, 7–20.
- van Hinsbergen, D.J., Steinberger, B., Doubrovine, P., Gassmöller, R., 2011. Acceleration-deceleration cycles of India–Asia convergence: roles of mantle plumes and continental collision. *J. Geophys. Res.* 116, B06101. doi:[10.1029/2010JB008051](https://doi.org/10.1029/2010JB008051).
- van Hinsbergen, D., Kapp, P., Dupont-Nivet, G., Lippert, P., DeCelles, P., Torsvik, T., in press. Restoration of Cenozoic deformation in Asia, and the size of Greater India. *Tectonics*. doi:[10.1029/2011TC002908](https://doi.org/10.1029/2011TC002908).
- Windley, B.F., Allen, M.B., 1993. Mongolian plateau: evidence for a late Cenozoic mantle plume under central Asia. *Geology* 21, 295–298.
- Yin, A., Harrison, T.M., 2000. Geologic evolution of the Himalayan–Tibetan orogen. *Ann. Rev. Earth Planet. Sci.* 28, 211–280.
- Zhang, Z.-K., Wang, M., Gan, W., Bürgmann, R., Wang, Q., Niu, Z., Sun, J., Wu, J., Hanrong, S., Xinzao, Y., 2004. Continuous deformation of the Tibetan Plateau from global positioning system data. *Geology* 32, 809–812.
- Zhong, S., Zuber, M.T., Moresi, L., Gurnis, M., 2000. Role of temperature-dependent viscosity and surface plates in spherical shell models of mantle convection. *J. Geophys. Res.* 105, 11 063–11,082..

# **Supplementary material for:**

## ***Mantle conveyor beneath the Tethyan collisional belt***

**Becker, T. W. and Faccenna, C., *Earth Planet Sci. Lett.*,**

**doi:10.1016/j.epsl.2011.08.021, 2011.**

**Thorsten W. Becker \***

*Department of Earth Sciences, University of Southern California, Los Angeles, CA*

**Claudio Faccenna**

*Dipartimento Scienze Geologiche, Università Roma TRE and IGAG, CNR Rome*

---

## **1 Methods**

The surface mechanical boundary conditions for most of our models are shear stress free (free slip), such that plate velocities are driven self-consistently by density contrasts within the mantle (Ricard and Vigny, 1989). The lithosphere in our models is defined rheologically as a relatively stiff layer from the surface to 100 km depth that is “broken” by weak zones of reduced viscosity, as in previous modeling (e.g. King and Hager, 1990; King et al., 1992; Zhong et al., 2000; Yoshida et al., 2001; Faccenna and Becker, 2010). The location of the weak zones used for most models (Fig. 2A) was assigned for the major plate boundaries following the NUVEL-1 geometry, and, for the case of Asia, located at the boundary of the actively deforming region (e.g. England and Molnar, 2005). All velocities are plotted in an Eurasia fixed reference frame (from a best-fit of the velocities within that plate, which typically show large intraplate deformation), and the core-mantle boundary is set to free-slip.

The numerical solution method is based on the finite element, CitcomS approach (Moresi and Solomatov, 1995; Zhong et al., 2000; Tan et al., 2006) with our minor modifications as discussed in Becker (2006) and Faccenna and Becker (2010).

---

\* Address: Department of Earth Sciences, University of Southern California, MC 0740, 3651 Trousdale Pkwy, Los Angeles, CA 90089–0740, USA. Phone: ++1 (213) 740 8365, Fax: ++1 (213) 740 8801

Email address: twb@usc.edu (Thorsten W. Becker).

We have verified that individual models have converged to a stable velocity solution in the presence of lateral viscosity variations. All results shown here have a mesh resolution of  $\sim 17$  km and  $\sim 26$  km in the horizontal and vertical direction, respectively. Resolution tests indicate that model velocities are stable to within a few percent under successive mesh refinement. The numerical resolution employed is therefore sufficient such that the model uncertainties are mainly due to imperfect knowledge of the input models, such as tomography velocity structure, and not due to computational limitations.

As described in Faccenna and Becker (2010), the instantaneous topographic deflection due to mantle flow (“dynamic topography”) was computed by dividing the radial normal stresses at the surface, as predicted by the flow model, by the product of gravitational acceleration ( $10 \text{ m/s}^2$ ) and density contrast between the mantle (density  $\rho_m = 3350 \text{ kg/m}^3$ ) and air over land, and the contrast between mantle and seawater (density  $\rho_w = 1020 \text{ kg/m}^3$ ) over water, a standard approximation. The residual topography to which we compare was inferred from crustal models by correcting the observed topography for the expected isostatic topography given the density and crustal thickness of the model CRUST2.0 (Bassin et al., 2000). All topography estimates have short wavelength structure removed by convolution with a Gaussian smoothing filter of 250 km diameter and are then shown after removal of any region-wide average topography.

## 2 Tests with different tomography models

We test the effect of using different seismic tomographic models, as shown in Fig. S1, for inferring mantle density structure and the resulting flow (Figs. S2 and S3). Our reference mantle density model as used for the flow computations shown in Figs. 2 and 3 is based on the global, composite  $S$  wave SMEAN model (Becker and Boschi, 2002) (Fig. S1A), with anomalies in the cratonic regions above 250 km removed. Alternative tomography models explored include the upper mantle SV model LH08 (Lebedev and van der Hilst, 2008), merged with SMEAN in the lower mantle (Figs. S1B and S3), and the higher resolution, global  $P$  model MITP08 (Li et al., 2008) (Figs. S1C and S2). For LH08, we correct for the presumably depleted nature of cratons by adding positive compositional buoyancy to the otherwise thermally dense (from tomography) regions within cratons.

The effect of one particular assumption for lateral variations in viscosity on the flow predictions are shown in Fig. S4, where continental keels down to 250 km (from the 3SMAC mode Nataf and Ricard, 1996) were assigned to be more viscous than the mantle by a factor of 100, and temperature-dependent viscosity was applied elsewhere following the simplified rheological description

$$\eta(T) = \eta_0 \exp(E(T_0 - T)) \quad (1)$$

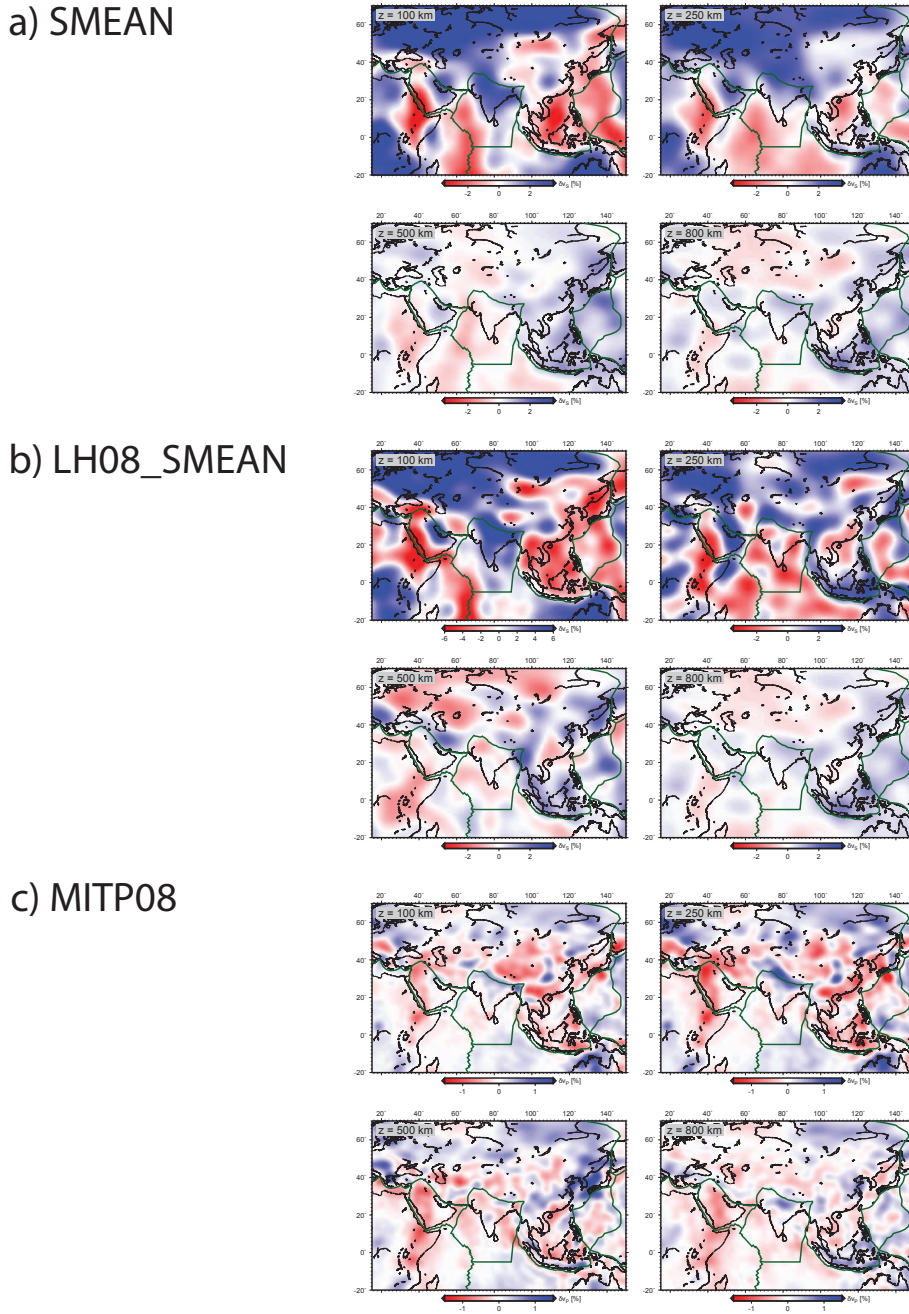


Fig. S1. Comparison of velocity anomaly maps of tomographic models used. A) Reference, global composite  $S$  wave model, SMEAN (Becker and Boschi, 2002); B) Upper mantle SV model LH08 (Lebedev and van der Hilst, 2008), merged with SMEAN in the lower mantle; C) Global, high resolution  $P$  wave model MITP08 (Li et al., 2008), all shown at 150, 250, 550 and 950 km depths.

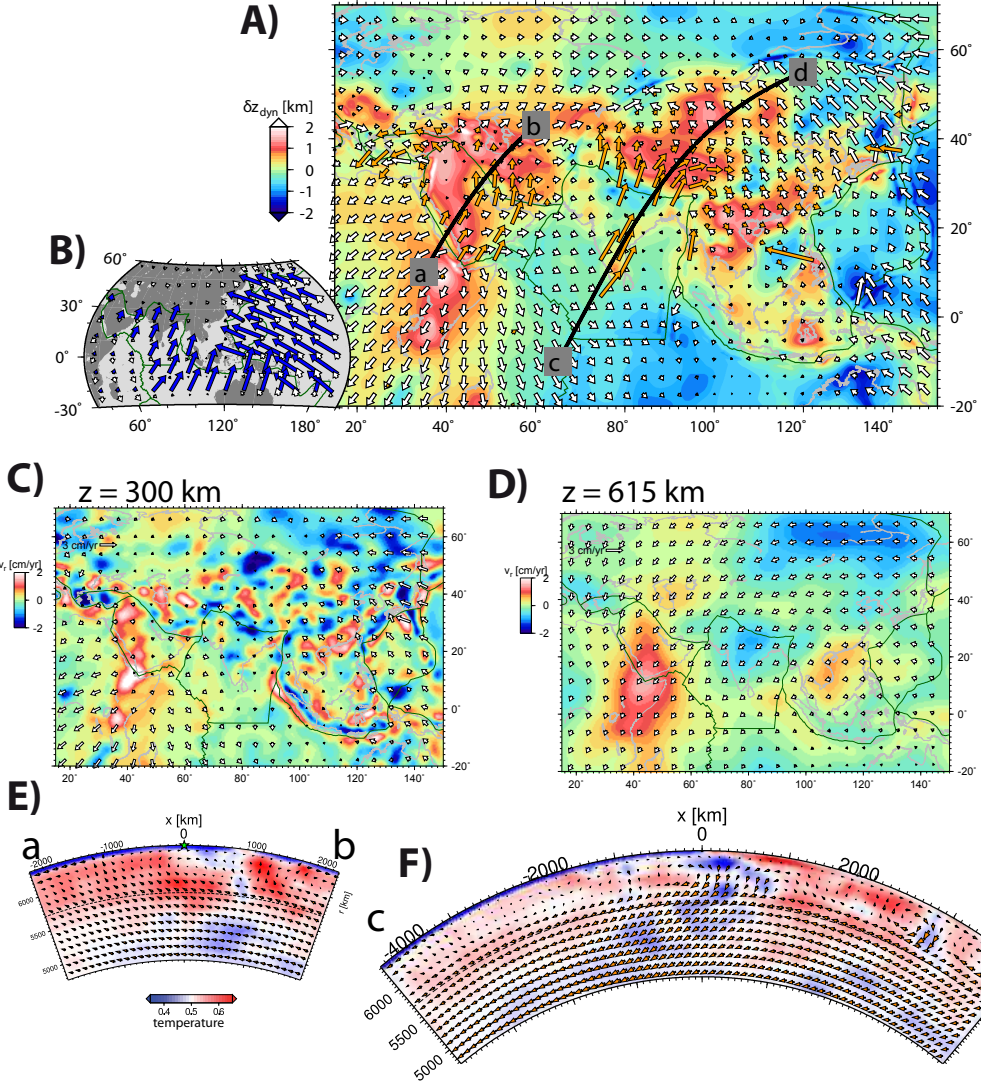


Fig. S2. Additional flow solution based on different tomography, the temperature structure is now inferred from the MITP08 tomography model (Li et al., 2008) (Fig. S1C). A) Predicted surface velocities and dynamic topography (boundary in green) of the Tethyan plate system (white vectors), geodetic velocities (orange), all shown in a best-fit, Eurasia fixed reference frame. B) Global predicted (blue arrows) and observed (white arrows, NUV-EL1A) large-scale velocities; C) Horizontal (white vectors) and vertical flow (background shading) field at 300 km and 615 km depth. Cross-sections from Afar to Iran (E) and from the Carlsberg ridge to Central Asia (F) (trace of cross section as in A), with non-dimensional temperature in the background. Compare with Figs. 2 and 3 in main text.

where  $\eta_0$  is the mean layer viscosity,  $T_0$  a reference temperature (the mean layer temperature),  $T$  the non-dimensional temperature as depicted in the cross-sectional figures and inferred from tomography, and  $E$  the Frank-Kamenetskii parameter (here  $E = 10$ ) (see, e.g., Ghosh et al., 2010, for details).

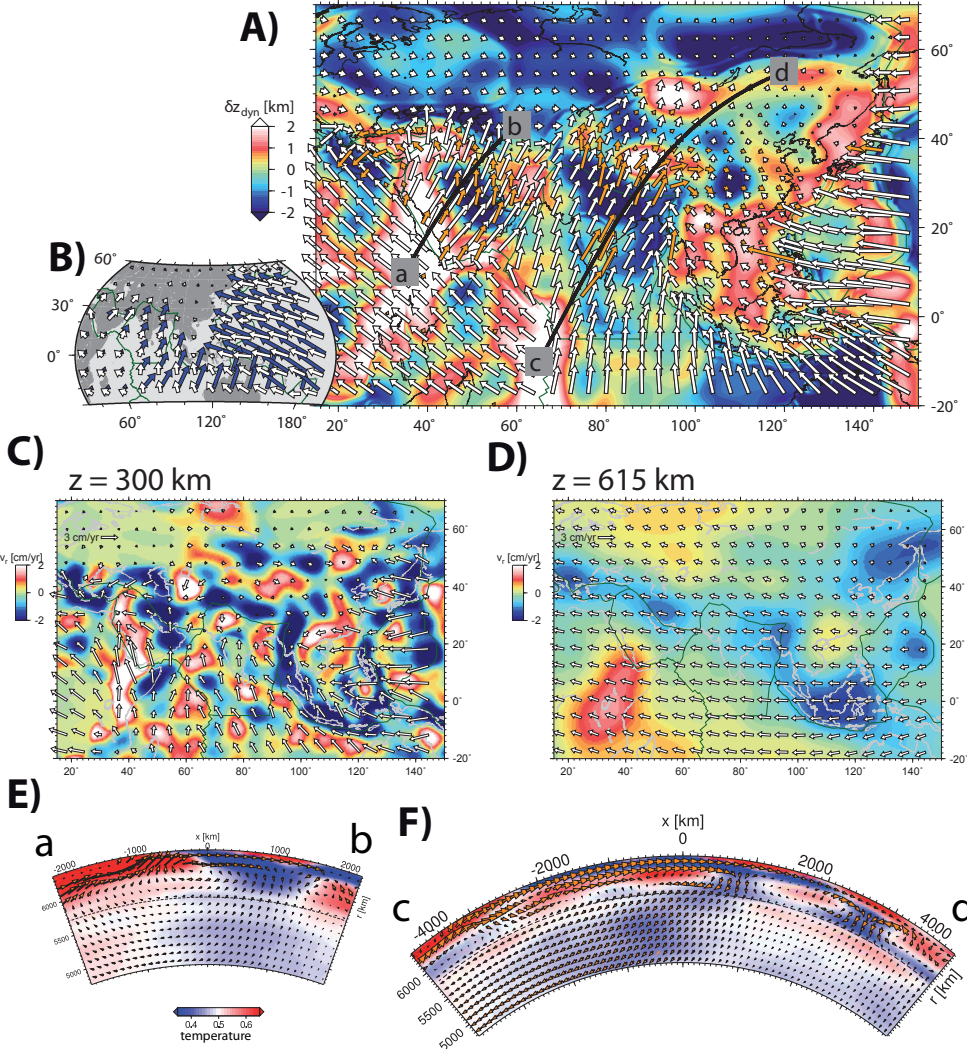


Fig. S3. Additional flow solution based on the SV wave tomography model LH08 (Lebedev and van der Hilst, 2008) (Fig. S1B). All plots shown depict the same quantities as in Fig. S2, see there for explanation.

### 3 Different components of tomography

To test the contributions from different components of the mantle system, we conducted several tests, including partitioning of the tomographic models. Firstly, Fig. S5A shows a more extensive approach in masking out any “cold” contributions underneath the continental lithosphere. There, compositional anomalies might be expected to be erroneously mapped into density by simple scalings of tomographic velocity. The reference model already had cratonic regions from Nataf and Ricard (1996) set to zero above 250 km. By comparing Figs. S5A and Fig. 2C, it can be seen that further removal of negatively buoyant structure in the continental litho-

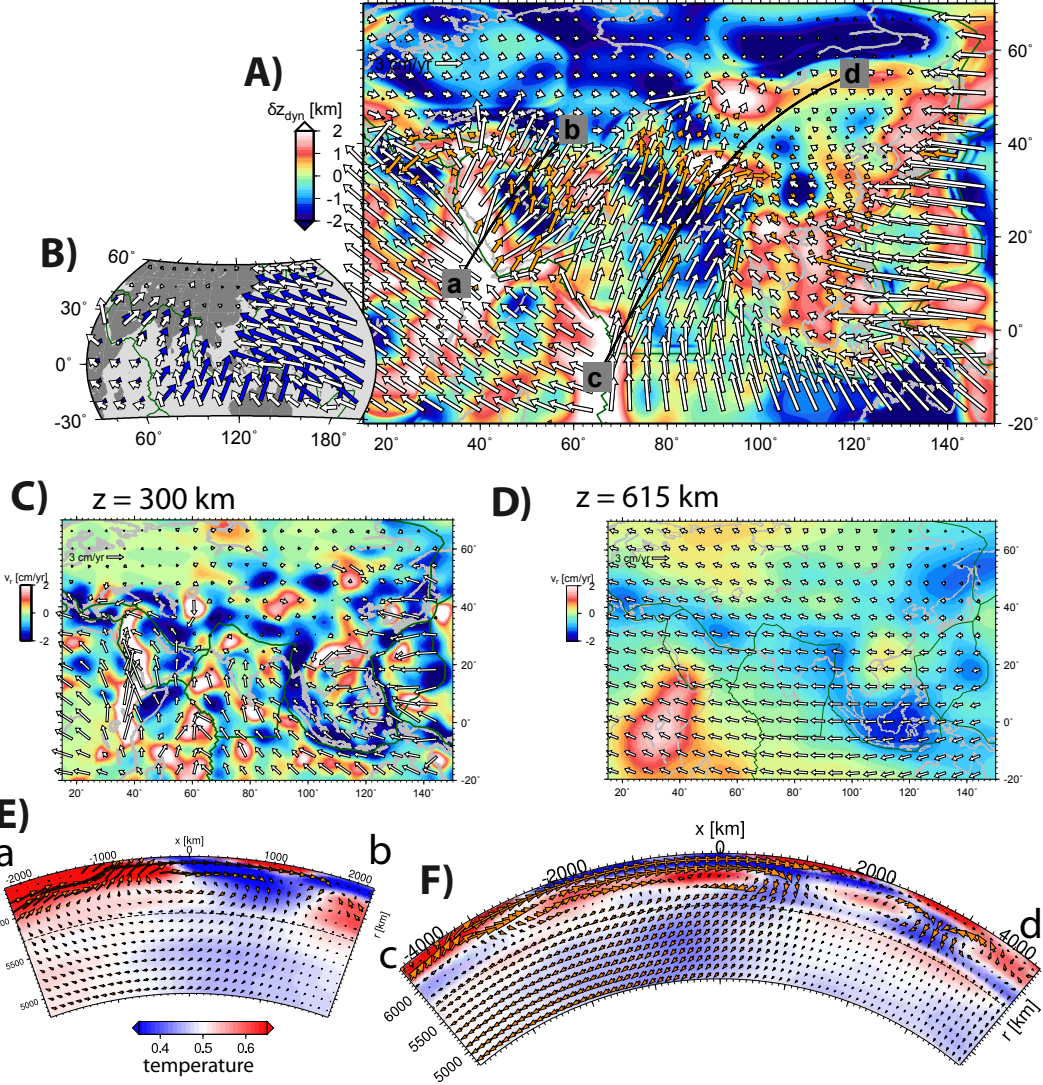


Fig. S4. Additional flow solution for reference model (as in Fig. 2) but including stiff keel beneath cratons and lateral viscosity variations as inferred from temperature (Frank Kamenetski approximation). All plots shown depict the same quantities as in Fig. S2, see there for explanation.

sphere does not affect the model in a major way. However, the masking of fast, shallow structure does remove some downwellings, such as underneath Arabia and in the immediate vicinity of the India-Eurasia plate boundary. The result is a moderate reduction of India plate motion, to  $\sim 80\%$  of the reference when evaluated in the center of the plate.

Secondly, Fig. S5B shows results when all negative (“hot”) anomalies from tomography are removed. Such a test is not equivalent to removing the effect of all upwellings, however. Since our approach does not consider hydrostatic pressure or compressibility effects, only the density anomalies after removal of a layer aver-

age matter for driving flow. This means that relative to any cold anomalies, there are broad regions of relatively hot material, such as underneath most oceanic plates. The resulting effects can be seen, for example, in positive dynamic topography over the spreading-center proximal regions (Fig. S5B). Velocities for India are  $\sim 60\%$  of the reference model. Thirdly, flow due to hot anomalies only is shown in Fig. S5C. Plate motions are reduced for the resulting, fairly localized upwellings and very broadly distributed downwellings; India moves at  $\sim 35\%$  of the reference model. These results imply that broad-scale upwellings and downwellings are the largest components of the conveyor belt, but localized, active upwellings such as underneath Afar contribute a significant component.

#### 4 Tests with different plate boundaries

Weak zone location, viscosity reduction and width are expected to affect the direction and amplitude of plate motions (e.g. King and Hager, 1990; Zhong et al., 2000; Yoshida et al., 2001). To demonstrate that our general conclusions are independent of those effects and the specific choices of the weak zone geometry used for most models (shown in Fig. 2A), we show surface velocities and dynamic tomography for two additional models in Fig. S6. Fig. S6A has the same weak zone geometry as the reference models, but the weak zone thickness is reduced from 300 to 150 km width. Comparison with the reference model shows that predicted dynamic topography and directions of plate motions are very similar for the thin weak zone model, whereas amplitudes of motions, such as for India, are slightly reduced. Fig. S6B uses the same width weak zones as in the reference, but the plate boundaries of Bird (2003) rather than the geologically motivated geometry adopted by us for all other models. Again, dynamic topography is only affected marginally by this change. However, plate motions are modified, particularly in regions where plates are now subdivided into smaller micro-plates, such as Africa and south-east Asia. The motions of Anatolia and India, for example, are sped up in the Bird (2003) plate boundary model, and there is less intraplate deformation in Tibet compared to the reference model. The decoupling of Nubia from Africa leads to overall more easterly trending velocities within India and the Eurasian plate. However, the broad-scale motions are consistent with the reference model and the arguments set forth in the main text.

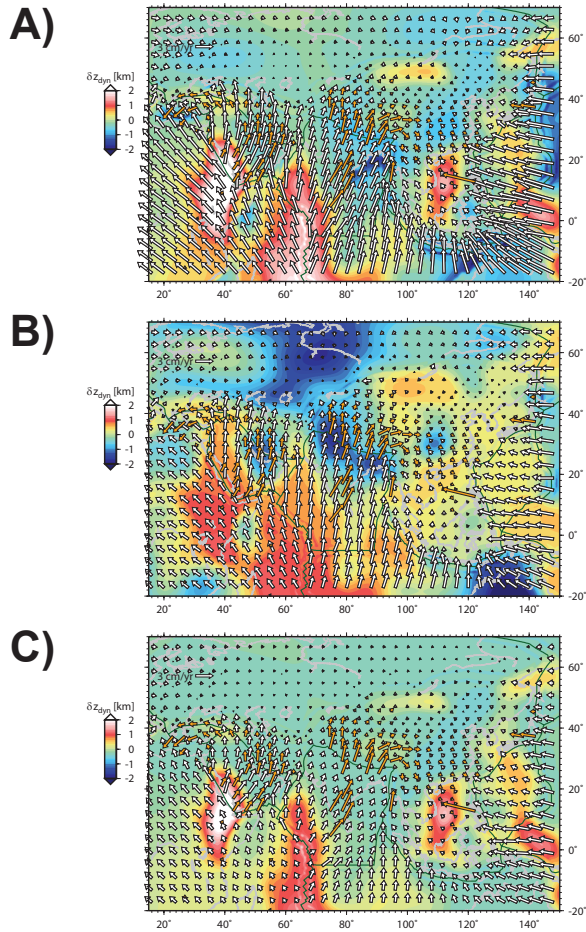


Fig. S5. Additional flow solutions, showing surface velocities and dynamic topography, for the reference model (as in Fig. 2C) but, A), setting positive (“cold”) tomographic velocity anomalies underneath all continental regions (from Nataf and Ricard, 1996) (not just cratons) above 250 km to zero; B) setting all negative (“hot”) velocity anomalies to zero in the tomographic model; and, C), setting all cold anomalies in tomography to zero.

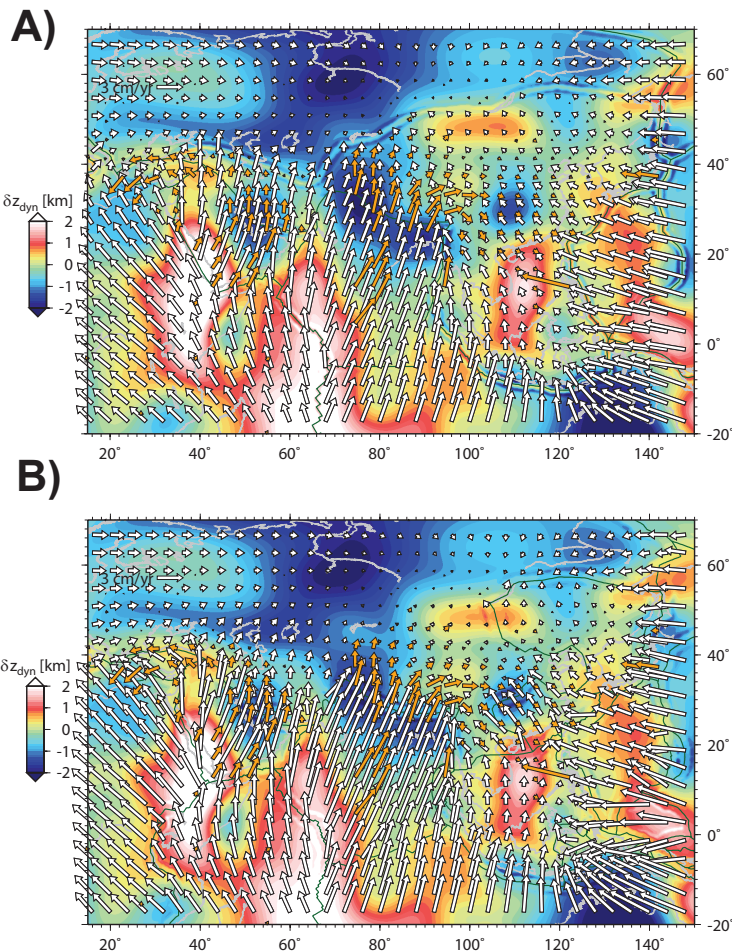


Fig. S6. Additional flow solutions, showing surface velocities and dynamic topography (as in Fig. 2C), for the reference model but, A), using thinner (150 km instead of 300 km wide) weak zones, and, B), using same width weak zones but along the plate boundaries from Bird (2003) instead of the geometry shown in Fig. 2A (see green lines).

## References

- Bassin, C., Laske, G., Masters, G., 2000. The current limits of resolution for surface wave tomography in North America (abstract). *Eos Trans. AGU* 81, F897.
- Becker, T. W., 2006. On the effect of temperature and strain-rate dependent viscosity on global mantle flow, net rotation, and plate-driving forces. *Geophys. J. Int.* 167, 943–957.
- Becker, T. W., Boschi, L., 2002. A comparison of tomographic and geodynamic mantle models. *Geochem., Geophys., Geosys.* 3, 1. doi:10.1029/2001GC000168.
- Bird, P., 2003. An updated digital model of plate boundaries. *Geochem., Geophys., Geosys.* 4. doi:10.1029/2001GC000252.
- England, P., Molnar, P., 2005. Late Quaternary to decadal velocity fields in Asia. *J. Geophys. Res.* 110, B12401. doi:10.1029/2004JB003541.
- Faccenna, C., Becker, T. W., 2010. Shaping mobile belts by small-scale convection. *Nature* 465, 602–605.
- Ghosh, A., Becker, T. W., Zhong, S., 2010. Effects of lateral viscosity variations on the geoid. *Geophys. Res. Lett.* 37, L01301. doi:10.1029/2009GL040426.
- King, S. D., Gable, C. W., Weinstein, S. A., 1992. Models of convection-driven tectonic plates: a comparison of methods and results. *Geophys. J. Int.* 109, 481–487.
- King, S. D., Hager, B. H., 1990. The relationship between plate velocity and trench viscosity in Newtonian and power-law subduction calculations. *Geophys. Res. Lett.* 17, 2409–2412.
- Lebedev, S., van der Hilst, R. D., 2008. Global upper-mantle tomography with the automated multimode inversion of surface and S-wave forms. *Geophys. J. Int.* 173, 505–518.
- Li, C., van der Hilst, R. D., Engdahl, E. R., Burdick, S., 2008. A new global model for P wave speed variations in Earth's mantle. *Geochem., Geophys., Geosys.* 9, Q05018. doi:10.1029/2007GC001806.
- Moresi, L. N., Solomatov, V. S., 1995. Numerical investigations of 2D convection with extremely large viscosity variations. *Phys. Fluids* 7, 2154–2162.
- Nataf, H.-C., Ricard, Y., 1996. 3SMAC: An *a priori* tomographic model of the upper mantle based on geophysical modeling. *Phys. Earth Planet. Inter.* 95, 101–122.
- Ricard, Y., Vigny, C., 1989. Mantle dynamics with induced plate tectonics. *J. Geophys. Res.* 94, 17,543–17,559.
- Tan, E., Choi, E., Thoutireddy, P., Gurnis, M., Aivazis, M., 2006. GeoFramework: Coupling multiple models of mantle convection within a computational framework. *Geochem., Geophys., Geosys.* 7. doi:10.1029/2005GC001155.
- Yoshida, M., Honda, S., Kido, M., Iwase, Y., 2001. Numerical simulation for the prediction of the plate motions: effects of lateral viscosity variations in the lithosphere. *Earth Planets Space* 53, 709–721.
- Zhong, S., Zuber, M. T., Moresi, L., Gurnis, M., 2000. Role of temperature-dependent viscosity and surface plates in spherical shell models of mantle con-

vection. *J. Geophys. Res.* 105, 11,063–11,082.